Supporting Information. Shocket, Marta, Daniela Vergara, Andrew Sickbert, Jason Walsman, Alexander Strauss, Jessica Hite, Meghan Duffy, Carla Cáceres, and Spencer Hall. (2018) Parasite rearing and infection temperatures jointly influence disease transmission and shape seasonality of epidemics. *Ecology*.

APPENDIX S1

In this appendix, we first describe the lab assay methods ([A] foraging rate assay and [B, C] infection rate assays) in greater detail. Second, we describe estimation of the parameters for the transmission model in greater detail. Third, we show the empirically measured transmission rate (β) with error bars (Fig. S1). Fourth, we explain several aspects of the epidemic simulations. More specifically, we (A) derive the equation for average rearing temperature of spores (T_R), (B) give the temperature-dependent parameterizations used for non-transmission traits (Table S1), (C) show the lag between past and current temperature in several scenarios (Fig. S2), (D) show data from a field survey of lakes that inspired the cooling scenarios considered in Fig. 5 (Fig. S4), and (E) provide a more thorough explanation for changes in the timing of epidemics (Fig. S4). Finally, we discuss why rearing effects can be important, even when there is no difference between parasite rearing and exposure/infection temperatures, using an illustration with some hypothetical experiments. This explanation also illustrates some considerations for designing experiments to measure rearing effects.

(1) Lab Assay Methods

All lab assays used a single clonal genotype of host isolated from a lake in Michigan (USA). Unless otherwise noted, hosts were kept in batch cultures under standard conditions (filtered lake water changed weekly, starting densities of 40-50 individuals per L, fed 1.0-2.0 mg dry mass / L of a nutritious [relative to natural algal assemblages in lakes] alga [either *Scendesmus sp.* rr *Ankistrodesmus sp.*] daily).

(A) Foraging Rate Assay

We measured foraging rate by comparing the fluorescence of ungrazed and grazed algae (Sarnelle and Wilson 2008, Penczykowski et al. 2014b). Hosts were cultured in constant temperature environments at 16, 18, 21, 24, and 27°C. For the assay, twenty-two individuals were selected from each temperature that spanned a size gradient including adults, large juveniles, and small juveniles. The hosts were transferred individually into centrifuge tubes containing 15 ml of filtered lake water and 1.0 mg dry mass / L algae. We also included 11 control tubes for each temperature that contained algae only. The tubes were returned to the constant temperature environments, kept dark, and inverted every 30 minutes to resuspend algae. After grazing for 8.5 hours, hosts were removed and measured (for body length, L: eye to base of tail spine at 50X). We measured *in vivo* fluorescence of the remaining algae in the grazed tubes, as well as the ungrazed control tubes (Turner Trilogy Laboratory Fluorometer).

(B) Infection Assay for Transmission Model

We measured transmission rate (β) at factorial combinations of parasite rearing (T_R) and exposure/infection (T_{EI}) temperatures using an infection assay. We reared spores at four temperatures (T_R = 15, 18, 20, and 22°C) and used them to generate infections at five temperatures (T_{EI} = 15, 18, 20, 22, and 25°C) for 20 total rearing-exposure/infection temperature combinations. Hosts were initially cultured at 20°C. Female adult hosts were placed in fresh lake water and offspring were harvested after 24-hours. Offspring were grown collectively for five days at 20°C (to control for body size at parasite exposure). On day 6, we measured the body size of a subset of hosts with a dissecting microscope (50X, average body length = 1.5 mm), divided hosts into exposure/infection temperature treatments, and moved them to the appropriate temperatures for the remainder of the experiment. For each treatment, twelve replicate beakers (six hosts per beaker) were filled with 100 ml of filtered lake water and exposed to a moderate spore dose (100 spores / ml) for 24 hours. All hosts were kept in their exposure/infection temperature environment and fed daily until visual diagnosis (20-50X) for infection (10-20 days post-exposure). For each treatment, we used maximum likelihood to estimate the transmission rate from the proportion infected (see *Estimating transmission rate [β]*).

(C) Infection Assay with Field-Collected Spores

Hosts were cultured at room temperature (~21°C). On November 25th, we individually exposed six-day-old large, adult hosts (L ≈ 1.5 mm) to spores in 15 ml tubes. For each lake-date, 48 hosts were split between two spore doses (50 and 150 spores/ml; 24 hosts exposed to each dose). The next day, all hosts in a given dose-lake-date treatment were moved to a single flask with fresh lake water. The assay was conducted at a single exposure/infection temperature (room temperature, ~21°C). Ten days later, we diagnosed the infection status of the hosts and calculated the proportion of hosts infected for each treatment. Uninfected hosts were re-examined on day 14. All hosts were fed 1.0 mg dry mass / L of *Ankistrodesmus sp.* daily.

(2) Estimating Parameters for Transmission Model

Estimating foraging rate, $f(T_{EI},L)$

We based our estimation on Shocket et al. (2018) but used maximum likelihood estimation in place of Bayesian inference. We assumed there was no algal growth during the dark assay. Thus, with only a single susceptible host (S) per tube, the differential equation for algae (A) consumed by the host at foraging rate (f) is:

$$\frac{dA}{dt} = -fSA \qquad \text{eq. S1}$$

Solving this exponential equation for resource density (A) yields:

$$A_{rem} = A_{init}e^{-fSt} \qquad \text{eq. S2}$$

where A_{rem} is the remaining algae observed in grazed tubes, A_{init} is the initial amount of algae (at time $t = 0$), S is the density of hosts (i.e., $1/V$, where V is the experiment volume), and t is the duration of the trial (~8.5 hours). We calculated foraging rate for each individual by log-transforming eq. S2 and solving for f:

$$f = \frac{\ln(A_{init}/A_{rem})}{St} \quad \text{eq. S3}$$

Estimating transmission rate (β)

We based our estimation on a simplified transmission model (Hall et al. 2006, Bertram et al. 2013), where susceptible hosts (S) are lost (and become infected) after contacting spores (Z) with transmission rate β:

$$\frac{dS}{dt} = -\beta ZS \quad \text{eq. S4}$$

We solve this equation for the remaining susceptible hosts (S_{rem}) after exposure time t_e yielding:

$$S_{rem} = S_{init}\, e^{-\beta Z t_e} \quad \text{eq. S5}$$

where S_{init} is the initial numbers of hosts in a beaker. We then use a binomial distribution to model the number of uninfected hosts in each beaker (*Infection Assay*) or for each tube exposure (*Infectivity Assay with Field-Collected Spores*). For the infection assay, the total number of hosts is number of animals in the beaker surviving to diagnosis (day 10). For the infectivity assay with field-collected spores, the total number of hosts is always one (i.e., a single animal with a binary outcome). In both cases, the probability of remaining uninfected (p_{uninf}) equals:

$$p_{uninf} = e^{-\beta Z t_e} \quad \text{eq. S6}$$

This probability is used in the binomial-based likelihood.

(3) Empirical Measurement of Transmission Rate (*β*) with Error Bars

The point estimates for transmission rate at each combination of rearing and exposure/infection temperature are presented here with 95% confidence intervals. (The same data are presented without confidence intervals in Fig. 2D.)

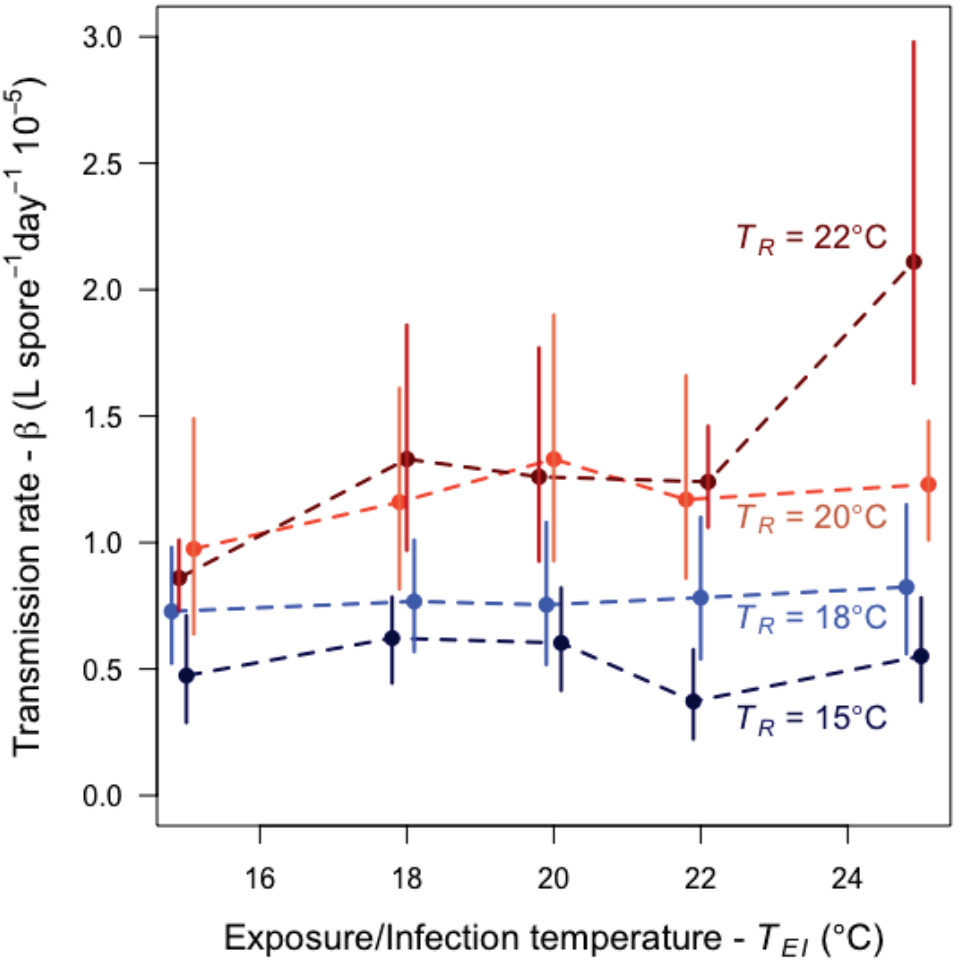

Figure S1: Transmission rate, $\beta(T_{EI},T_R)$ with confidence intervals: Empirical estimates from the infection assay data for each combination of rearing and exposure/infection temperature (seen also in Fig. 2D), with error bars showing 95% CIs generated from 10,000 bootstraps around each point estimate. Exposure/Infection temperature values are jittered for visual clarity.

(4) Epidemic Simulations

(A) Derivation of Average Rearing Temperature of Spores (T_R, eq. 3d)

In the dynamical model (eq. 3), the spore rearing temperature (T_R) is the average rearing temperature of all spores in the system. We track this quantity via "spore-degrees" (T_Z). The number of spore degrees is the sum of the rearing temperature of every spore present in the environment. Thus, T_R is defined as the number of spore degrees divided by the number of spores:

$$T_R = \frac{T_Z}{Z} \qquad \text{eq. S7}$$

As spores are added to the system (at rate $d_i\, I\, \sigma$), they add spore-degrees at that addition

rate multiplied by the current temperature ($d_i\ I\ \sigma\ T_{EI}$). As spores are removed from the system (at rate $m + f\ S\ I$), they remove spore-degrees at this removal rate multiplied by the average rearing temperature ($[m + f\ S\ I]T_R$).

Next, we calculate the derivative of T_R through time by applying the quotient rule to eq. S7:

$$\frac{dT_R}{dt} = \frac{d}{dt}\left(\frac{T_Z}{Z}\right) = \frac{(dT_Z/dt)\ Z - (dZ/dt)\ T_Z}{Z^2} \qquad \text{eq. S8}$$

We substitute the following quantities based on the fluxes of spores in the model (eq. 3c):

$$dT_Z/dt = d_i I \sigma T_{EI} - [m + f(S + I)]ZT_R \qquad \text{eq. S9a}$$

$$dZ/dt = d_i I \sigma - [m + f(S + I)]Z \qquad \text{eq. S9b}$$

And then simplify to reach:

$$\frac{dT_R}{dt} = \frac{d_i I \sigma (T_{EI} - T_R)}{Z} \qquad \text{eq. S10}$$

Intuitively, this result tracks changes in the mean rearing temperature of all spores in the environment. As epidemics progress, new spores in the environment are reared at colder temperatures. Change in mean rearing temperature is it is elevated by larger inputs of new spores ($d_i\ I\ \sigma$), which were reared recently. The impact of these new spores is weighted by the difference between their rearing temperature (T_{EI}) and the mean rearing temperature of the older spores (T_R). Additionally, it is slowed by higher densities of old spores (Z) that were reared at warmer temperatures and remain in the environment.

(B) Temperature-Dependent Parameterization for non-transmission traits

We used the temperature-dependent functions below to parameterize the dynamical model. Aside from spore infectivity and host foraging rate (u and f, respectively, which were fit in this study), functions were taken from Shocket et al. (2018). Spore yield (σ) was fit to values from high levels of high quality algal food resources (σ_{max}, from animals fed 2.0 mg/L dry weight of high quality algae daily). These spore yields are unrealistically high for epidemics in nature. Thus, we scaled that function by 0.15 in order to preserve the temperature-dependence, but obtain values that are similar to those we observe from animals in the field (~23,000 spores per host). The value for the density-dependence strength factor was taken from (Duffy et al. 2005).

Table S1: Traits (parameters, 'Par.') for the dynamical model (eq. 3). Coefficients (with 95% credible or confidence intervals) are given for traits or parameters fit as functions of temperature. The spore yield function was fit with temperature in degrees Celsius. All other functions were fit with temperature in Kelvin. The functions for spore infectivity (u) and host foraging rate (f) are from this study. The density dependence parameter © was taken from Duffy et al. (2005). All others were taken from Shocket et al. (2018).

Par.	Meaning (units)	Function Type	Function Coefficients (95% CIs)
b	host birth rate (day^{-1})	Derived function of T_{EI}: $b = r + d$	
r	host per capita growth rate (day^{-1})	Arrhenius function of T_{EI}: $r(T_{EI}) = r_{Ref} \cdot e^{T_A\left(\frac{1}{T_{Ref}} - \frac{1}{T_{EI}}\right)}$	$\boldsymbol{r_{Ref}}$ **= 0.325** (0.314 – 0.335) $\boldsymbol{T_A}$ **= 3,900** (3,210 – 4,610)
d	uninfected host death rate (day^{-1})	Arrhenius function of T_{EI}: $d(T_{EI}) = d_{Ref} \cdot e^{T_A\left(\frac{1}{T_{Ref}} - \frac{1}{T_{EI}}\right)}$	$\boldsymbol{d_{Ref}}$ **= 0.0118** ($6.72 \cdot 10^{-3}$ – 0.0187) $\boldsymbol{T_A}$ **= 13,000** (2,820 – 24,200)
c	Density dependence strength factor $(No./L)^{-1}$	Parameter does not vary with T	**c = 0.05**
u (eq. 2)	Per spore infectivity ($spore^{-1}$)	Linear function of T_{EI} and T_R: $u(T_C, T_P) = \alpha_{EI} T_{EI} + \alpha_R T_R + \alpha_I$	$\boldsymbol{\alpha_{EI}}$ **= -4.93 · 10^{-5}** (-10.3 – -1.08 · 10^{-5}) $\boldsymbol{\alpha_R}$ **= 8.99 · 10^{-5}** (6.89 – 12.1 · 10^{-5}) $\boldsymbol{\alpha_I}$ **= -0.0111** (-0.0245 – 0.00188)
f (eq. 1)	host foraging rate (L / day)	Arrhenius function of T_{EI} with power function of body length (L): $f(T_C, L) = L^{\gamma} \cdot \hat{f} \cdot e^{T_A\left(\frac{1}{T_{Ref}} - \frac{1}{T_{EI}}\right)}$	$\boldsymbol{\gamma}$ **= 2.18** (1.60 – 2.98) $\boldsymbol{\hat{f}}$ **= 5.36 · 10^{-3}** (3.70 – 6.75 · 10^{-3}) $\boldsymbol{T_A}$ **= 8,720** (4,800 – 12,600)
d_i	infected host death rate (day^{-1})	Arrhenius function of T_{EI}: $d_i(T) = d_{iRef} \cdot e^{T_A\left(\frac{1}{T_{Ref}} - \frac{1}{T_{EI}}\right)}$	$\boldsymbol{d_{iRef}}$ **= 0.0566** (0.0440 – 0.0706) $\boldsymbol{T_A}$ **= 5,390** (971 – 10,600)
σ	spore yield ($spores \cdot 10^4 / host$)	Quadratic function of T_{EI}: $\sigma(T) = 0.15\ (\alpha_2 \cdot {T_{EI}}^2 + \alpha_1 \cdot T_{EI} + \alpha_0)$	$\boldsymbol{\alpha_2}$ **= -0.149** (-0.242 – -0.0550) $\boldsymbol{\alpha_1}$ **= 6.42** (2.50 – 10.2) $\boldsymbol{\alpha_0}$ **= -53.2** (-92.0 – -13.9)
m	Background spore loss rate ($spores / day$)	Parameter does not vary with T	$\boldsymbol{m}$ **= 0.9**

(C) Lag Between Rearing and Exposure/Infection Temperature

For simulations using the sigmoidal temperature profile (designed to mimic what we typically observe in lakes with *D. dentifera*-*M. bicuspidata* epidemics), the difference between the rearing temperature of spores (T_R) and the exposure/infection temperature (T_{EI}) was negligible compared to the seasonal shifts in both temperatures. The maximum difference was either 0.17°C (for temperature-dependent f) or 0.16°C (for constant f), and occurred when the

slope of temperature was highest (Fig 4A). Even with extremely unrealistic parameters designed to maximize the lag between T_R and T_{EI} (spore loss rate [m] = 0.05, spore yield [σ] scaled to one-third of the value used in other simulations), the difference only increased to 1.3°C.

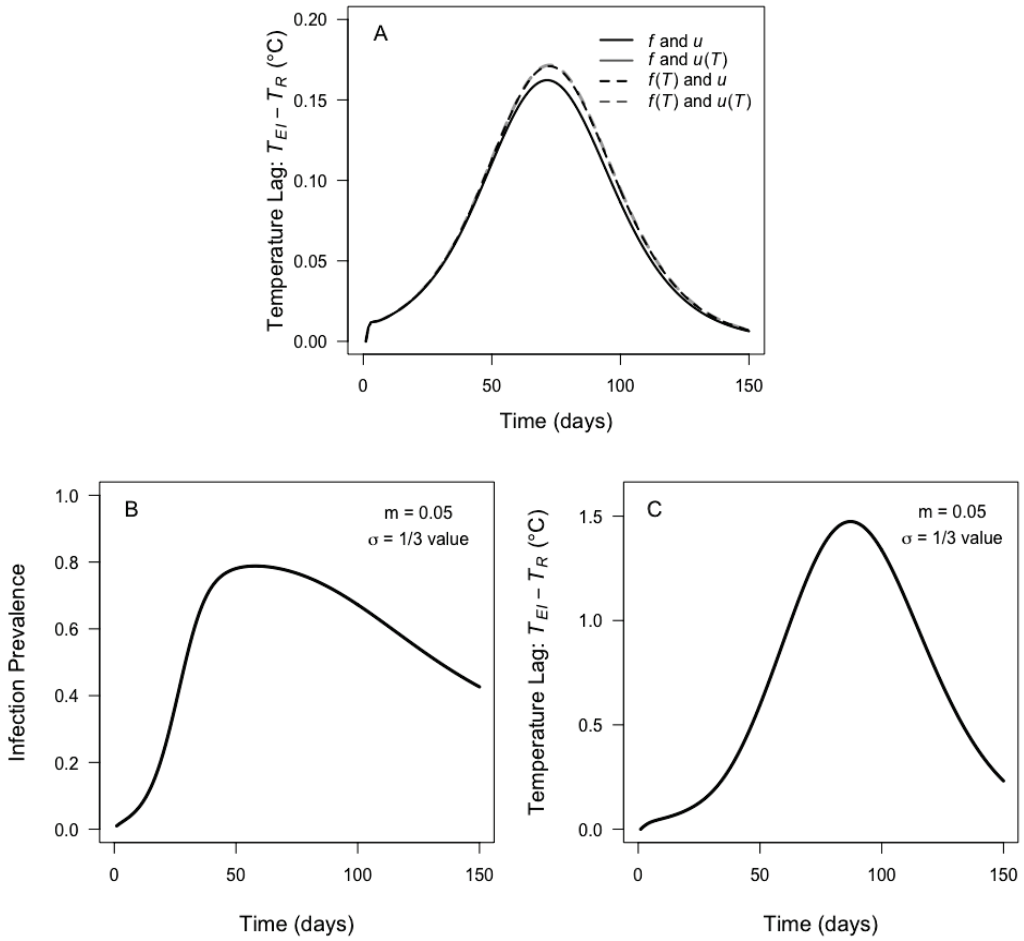

Figure S2: A) The lag between exposure/infection temperature (T_{EI}) and rearing temperature (T_R) for the four epidemic simulations in Figure 4. The lag was negligible compared to the seasonal shifts in both temperatures. For all simulations the difference peaked at either 0.16°C or 0.17 °C on day 72 (two days after the slope of T_{EI} was steepest). B) Epidemic dynamics and C) the lag between T_{EI} and T_R in simulations with unrealistic parameters designed to maximized the lag (spore loss rate [m] = 0.05, spore yield [σ] scaled to one-third of the value used in other simulations). The difference peaked at 1.5°C on day 87 (seventeen days after the slope of T_{EI} was steepest).

However, we can get larger lags if we use different temperature profiles. The lakes dominated by *D. dentifera* cool gradually because of the large volume of water and water's high heat capacity. However, sudden changes in temperature are possible in terrestrial and smaller-volume aquatic ecosystems. For a temperature profile with a sudden shift in exposure/infection temperature (and lower spore loss rate [m = 0.05]), the lag starts at the magnitude of the temperature shift and then declines gradually over time (Fig S3A,B). Furthermore, these lags can

impact transmission rate (Fig S3C) and infection dynamics (Fig S3D).

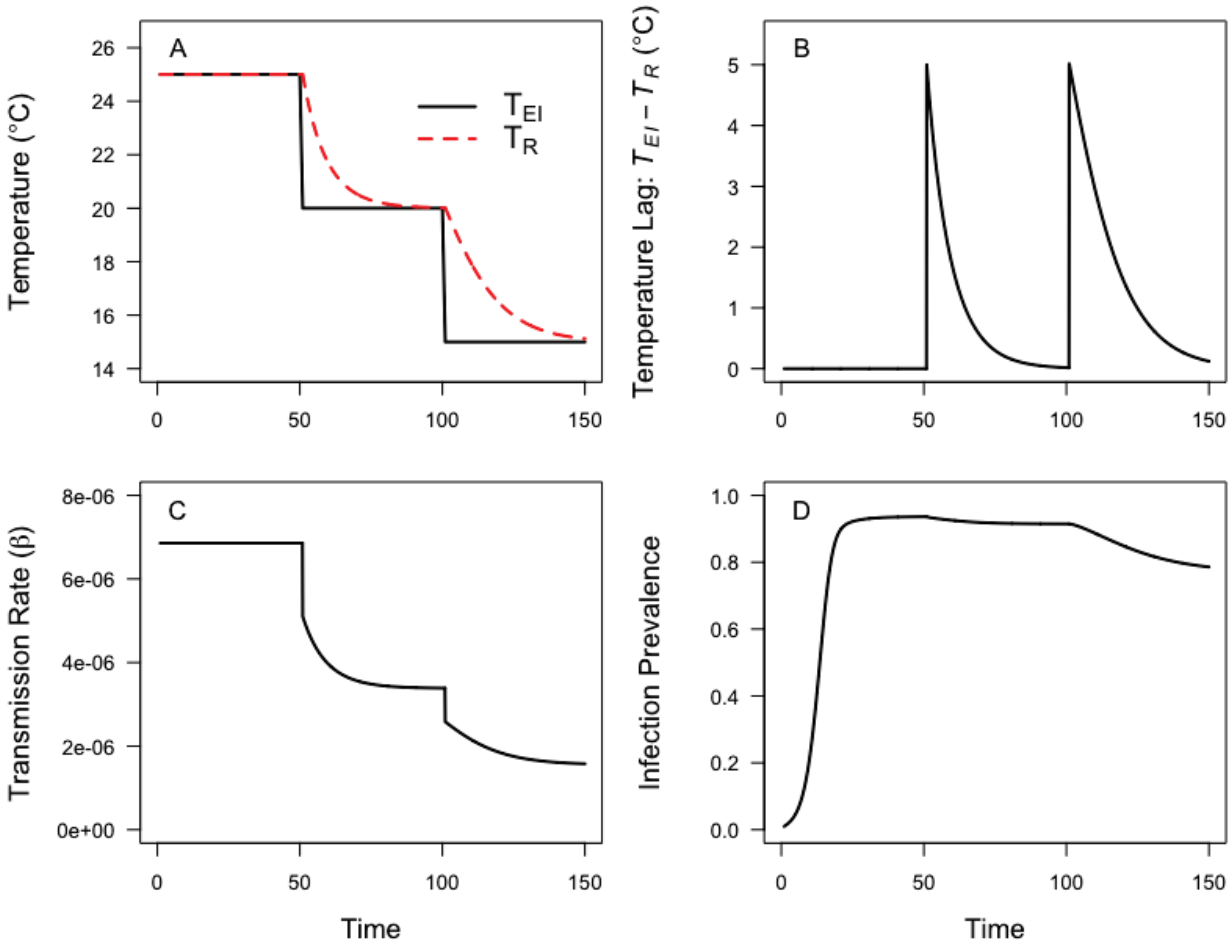

Figure S3: Simulations using a temperature profile with sudden 5°C shifts in temperature and spore loss rate [m] = 0.05 allow for a larger lag between exposure/infection temperature (T_{EI}) and rearing temperature (T_R). (A) The exposure/infection temperature (T_{EI}) and rearing temperature (T_R). (B) The lag between exposure/infection temperature (T_{EI}) and rearing temperature (T_R) now shows large spikes that decay over time, which also changes the trajectory of (C) transmission rate (β) and (D) infection prevalence.

(D) Cooling Patterns from Field Survey of Lakes

The different cooling scenarios in Fig. 5 were inspired by field data collected during a 7-year survey of lakes in southwestern Indiana (Greene and Sullivan counties). The number of lakes surveyed each year varied between 10 and 28, depending on available resources. Lakes were visited weekly (2009-2011) or bi-weekly (2012-2015) from August to December. At each visit, we measured lake water temperature data at 0.5 – 1 meter intervals with a Hydrolab multiprobe (Hach Environmental). We calculated weighted temperature as the effective temperature that hosts experience based on their daily migration patterns, under certain

assumptions (see Shocket et al. 2018). Cooling scenarios varied between lakes based on local-scale geography and lake physical structure (Fig. S4A). Shallower lakes (maximum depth < 10 M) were typically warmer than deeper lakes (maximum depth > 10 M). Cooling scenarios also varied between years for a single lake based on large-scale variation in climate (for example, Gambill: Fig. S4B). For example, starting temperature (T_{max} in the dynamical model) was warmer in 2010 and cooler in 2015 compared to most years. In 2011, cooling started earlier than usual (higher D in the dynamical model).

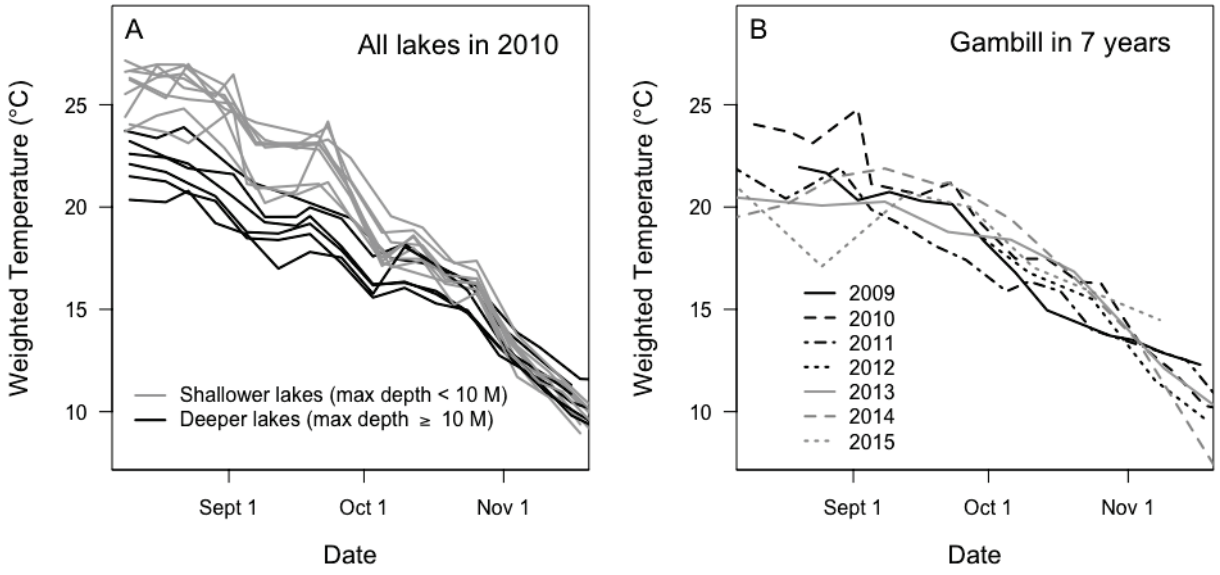

Figure S4: Examples of variation in cooling profiles between A) different lakes in a single year and B) a single lake in seven years. Lakes are in Greene and Sullivan Counties, Indiana, USA. All lakes contain focal hosts; some lakes experience epidemics of the fungal parasite. A) Lakes vary in weighted temperature (the effective temperature that hosts experience due to their daily migration patterns, see Shocket et al. 2018) based on their physical structure. Shallower lakes (maximum depth < 10 M) are typically warmer than deeper lakes (maximum depth > 10 M) during the first two-thirds of the epidemic season (higher T_{max} in the dynamical model). B) Temperature varies between different years in a single lake (Gambill) based on large-scale variation in climate.

(E) Explanation of Timing Changes

We can gain more insight into changes in peak timing of simulated epidemics. Although the patterns vary with the particulars of each cooling scenario, the underlying ideas driving all of the patterns are similar. Peak (maximum) prevalence largely reflects a timing cascade during epidemics. Take, for instance, variation in starting temperature (T_{max}; top row, Fig. S4.A-C). The timing is: first susceptible hosts, $S(t)$, are depleted to a minimum (Fig. S4.A), then infected hosts, $I(t)$, reach a maximum (Fig S4.B), then peak prevalence is reached shortly thereafter (Fig. S4.C; see also Fig. 5). The timing of minimum $S(t)$ usually – but not always – occurs after the temporal dynamic (solid lines) cross the minimal host requirement of the parasite, calculated at

equilibrium (i.e., the parasite's S^*; dashed lines; left row, Fig. S4.A,D,G; found numerically with a rootfinder). That minimal host requirement, i.e., the number of hosts needed to sustain the epidemic at equilibrium, increases as temperatures cool (through time, moving along the x-axis). This S^* remains higher when maximum temperatures (T_{max}) start cooler as well. Epidemics that start warmer can exhaust more hosts (i.e., plunge $S(t)$ lower) because transmission rate, β, is higher when it is warmer. (Although other thermally dependent traits also influence S^*, β is the key one). Next in the timing cascade: after susceptible hosts are depleted, infected host density, $I(t)$, reaches its maximum (middle column; Fig. S4.B,E,H). However, equilibrial infected density (I^*) drops through time with cooling, since colder temperatures support smaller epidemics. Hence, as the attractor I^* drops below $I(t)$, the epidemic falls. Essentially, temperature suppresses the interior epidemic attractor, eventually leading to a stable boundary (disease-free) equilibrium (through a transcritical bifurcation). Those shifts in attractor behavior pulls epidemics down towards parasite extinction, thereby causing epidemics to wane. The pattern of peak prevalence, p, closely mirrors the pattern of peak infected density, I (e.g., right column; Fig. S4.C,F,I).

With this logic in mind, the differing relationships between the timing of peak prevalence, p, and cooling parameters (T_{max}, D, and R) becomes more clear. The timing of peak prevalence (max p) shows a unimodal relationship with maximum temperature, T_{max} (top row, Fig. S4.A-C). That hump arises because, at high T_{max}, the epidemic burns through hosts quickly (with such high β; see the 25°C, dark grey line in Fig. S4.A). At intermediate T_{max}, it takes longer for the parasite to burn through its host. At low T_{max}, the epidemic actually hits the maximum epidemic size before S is depleted (i.e., S does not limit epidemics; e.g., the T_{max} = 19°C, light grey example in Fig. S4.A). The date parameter governing cooling, D, produces a simpler pattern (middle row; Fig. S4.D-F). Here, the delay in cooling due to higher (later) D allows the thermally-sensitive parasite to exhaust S to even lower levels. Meanwhile, at high D, S^* stays lower for longer (since infection risk remains higher during later season, and higher infection risk keeps S^* lower). Finally, as rate of cooling, R, increases, the relationship between timing of peak p and R is complex (bottom row, Fig. S4.G-I). Essentially, the pattern arises due to a race between depletion of hosts, $S(t)$, vs. the increase in S^* with cooling. The timing of that $S(t)$ vs. S^* race determines the concave up, unimodal relationship. Higher R (steeper cooling) enables a deeper plunge of S(t); at more intermediate R, S(t) catches S* a few days earlier as parameterized); at low R (more graduate cooling), the parasite cannot deplete S as low (so epidemics are a bit smaller) but the parasite can burn S longer (since $S(t)$ does not cross S^* until later; Fig. S4.G).

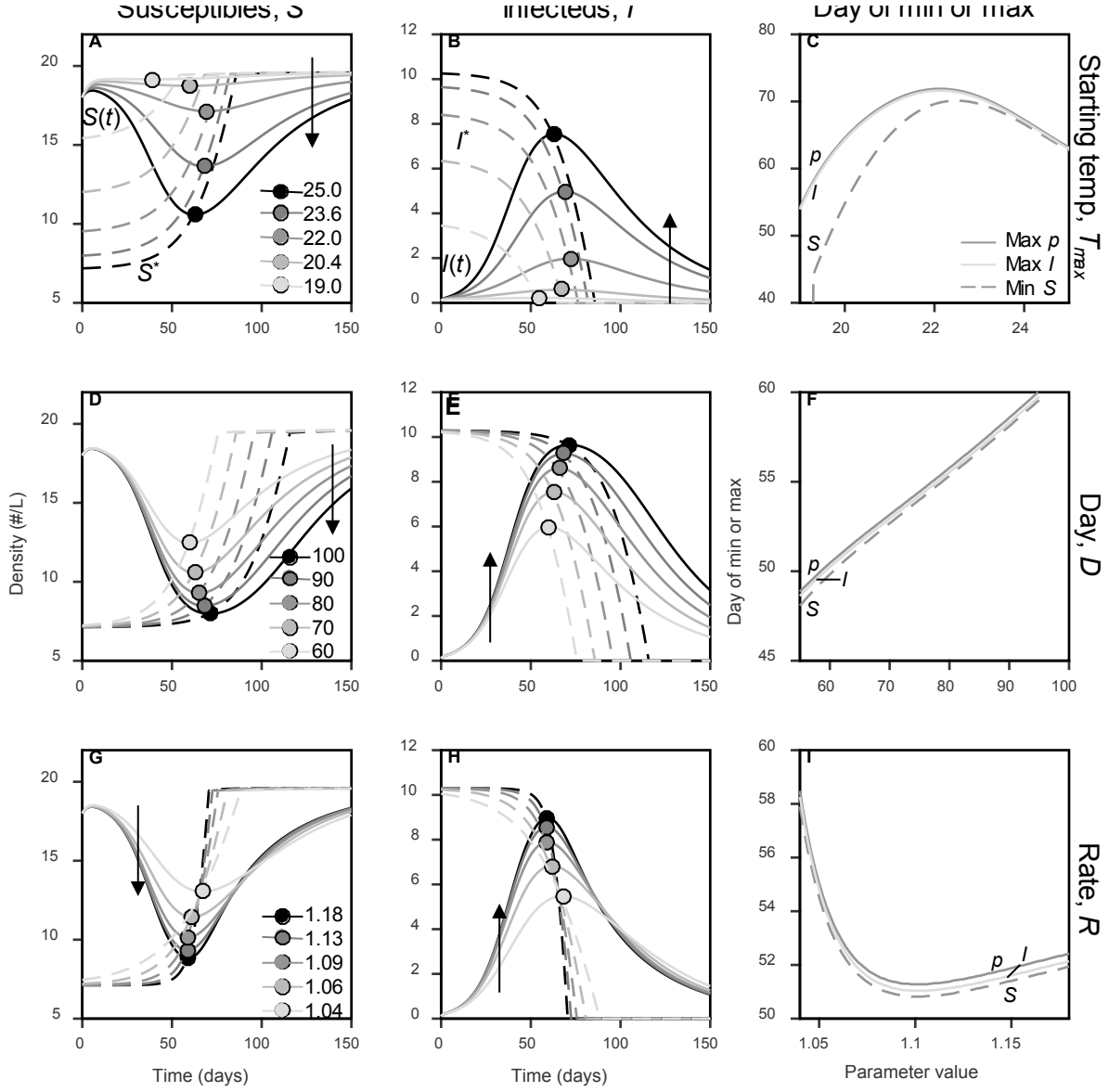

Figure S5:. An analysis of the timing of peak prevalence (max p). Timing of peak p reflects timing of depletion of susceptible hosts (S) to minimal host requirements (S^*) followed by the timing of peak infected density (I) at its intersection with equilibrial infected host density (I^*). Essentially, epidemics typically peak after they have depleted their susceptible hosts to S^*, and that depletion depends on rate of cooling of exposure/infection and rearing temperatures, T_{EI} and T_R, respectively, and their effect on transmission rate, β. Left column: susceptible host density through time, $S(t)$ (solid lines), and minimal host requirements, S^* (dashed lines). Middle column: infected host density through time, $I(t)$ (solid lines), and equilibrial infected density (dashed lines). Right column: timing of peak prevalence (p; solid dark grey), maximum infected density (I; solid light grey), and minimum susceptible density (S; dashed grey). Top row: variation in maximal (starting) temperature, T_{max}. Middle row: day of intermediate cooling, D. Bottom row: rate of cooling, R. Arrows point to warmer cooling scenarios (towards darker grey).

(5) The importance of rearing effects (and how to measure them) illustrated with hypothetical experiments

The most common question we encountered (even within our research group) while writing this paper was: if the population model shows there is no difference between parasite rearing temperature (T_R) and exposure/infection temperature (T_{EI}), does rearing temperature still matter? We've found that the answer to this question is best communicated through the following example using hypothetical experiments. The explanation also illustrates some important things to keep in mind when designing experiments to measure rearing effects.

The rearing effect matters *even if* both temperatures are the same because it is a *distinct biological mechanism* that acts through differences in spore quality. For instance, a typical lab experiment (#1) investigating temperature and infection rate would not be able to detect this mechanism because it only manipulates the exposure/infection temperature while creating infections with parasites from a common stock (i.e., a single rearing temperature). A better experiment (#2) could account for the rearing effect (but *not* measure it) by creating infections where the parasite rearing temperatures matched the exposure/infection temperatures. The best experiment (#3) is able to measure the rearing effect with a factorial combination of parasite rearing and exposure/infection temperatures. Experiment #2 would be sufficient to account for the rearing effect and make accurate predictions for what happens in nature in a system with no difference between T_R and T_{EI}—but only in hindsight after doing experiment #3! Only experiment #3 can tell you that experiment #2 is worth conducting in place of experiment #1. Furthermore, if the current environment matters, experiment #2 cannot accurately measure the magnitude of the rearing effect. In the *D. dentifera-M. bicuspidata* system, experiment #2 would find only a weak response of spore infectivity to temperature (e.g., as in Shocket et al. 2018). This miscalculation occurs because the negative effect of exposure/infection temperature masks the true magnitude of the rearing effect. Thus, ideally rearing effects should be measured using large, factorially-crossed experiments (which perhaps helps explain why they are understudied).

LITERATURE CITED

Bertram, C. R., M. Pinkowski, S. R. Hall, M. A. Duffy, and C. E. Cáceres. 2013. Trait-mediated indirect effects, predators, and disease: Test of a size-based model. Oecologia 173:1023–1032.

Duffy, M. A., S. R. Hall, A. J. Tessier, and M. Huebner. 2005. Selective predators and their parasitized prey: Are epidemics in zooplankton under top-down control? Limnology and Oceanography 50:412–420.

Hall, S. R., A. J. Tessier, M. A. Duffy, M. Huebner, and C. E. Cáceres. 2006. Warmer does not have to mean sicker: temperature and predators can jointly drive timing of epidemics. Ecology 87:1684–95.

Penczykowski, R. M., B. C. P. Lemanski, R. D. Sieg, S. R. Hall, J. Housley Ochs, J. Kubanek, and M. A. Duffy. 2014. Poor resource quality lowers transmission potential by changing foraging behaviour. Functional Ecology 28:1245–1255.

Sarnelle, O., and A. E. Wilson. 2008. Type III functional response in Daphnia. Ecology 89:1723–1732.

Shocket, M. S., A. T. Strauss, J. L. Hite, M. Šljivar, D. J. Civitello, M. A. Duffy, C. E. Cáceres, and S. R. Hall. 2018. Temperature Drives Epidemics in a Zooplankton-Fungus Disease System: A Trait-Driven Approach Points to Transmission via Host Foraging. The American Naturalist 191:435–451.